arXiv:1107.2279v1 [cond-mat.str-el] 12 Jul 2011

Magnetic interactions in iron superconductors revisited

M.J. Calderón, G. León, B. Valenzuela, and E. Bascones*
Instituto de Ciencia de Materiales de Madrid, ICMM-CSIC, Cantoblanco, E-28049 Madrid (Spain).

(Dated: July 13, 2011)

The magnetic interactions of iron superconductors are studied within the Hartree-Fock (HF) and Heisenberg descriptions of the same five orbital model. The experimentally observed $(\pi, 0)$ order is more stable in the HF approximation than in the Heisenberg one. Due to virtual transitions involving filled orbitals, the first and second nearest neighbor exchange constants J_1 and J_2 of the strong-coupling description become ferromagnetic (FM) at large Hund's coupling. Ferromagnetic tendencies are enhanced with electron doping and suppressed with hole doping, the electron-hole asymmetry being less important for small interactions. The Hartree-Fock phase diagram lacks a ferromagnetic phase but includes a double stripe (DS) state. In undoped compounds this state is unstable towards phase separation (PS), but it can be stabilized with electron-doping. In both descriptions, (π, π) antiferromagnetic order appears on the phase diagram correlated with an unusual orbital reorganization. A non-monotonous dependence of J_1 and J_2 on the Fe-As-Fe angle is found. The implications of our findings for the magnetic state of iron superconductors are discussed.

PACS numbers: 75.10.Jm, 75.10.Lp, 75.30.Ds

The origin of the magnetism in iron superconductors, believed to be key to explain their high-Tc superconductivity, is still unsettled. Most iron pnictides order with $(\pi, 0)$ momentum, AF in the x-direction and FM in the y-direction[1, 2]. The itinerant versus strong coupling origin of magnetism is at the heart of the debate. The itinerant picture relies on the metallicity of the AF and an approximate nesting between hole and electron pockets[3–5]. In the strong coupling description, localized spins interact AF with their first and second nearest neighbors[6, 7]. Clasically, a $(\pi, 0)$ state arises when $J_2 > J_1/2$. A large J_2 was justified by the As-mediated exchange between Fe atoms. In contrast, FeTe orders FM along one of the diagonals and AF along the other one in a double stripe pattern. A large exchange interaction to third nearest neighbors J_3 has to be introduced to explain the stability of this state within a localized picture [8]. A relation between its magnitude and the Fe-Te layer geometry has been claimed [9]. No nesting features compatible with this ordering have been observed [10].

Little is known about the value of the exchange constants. In strongly correlated multiorbital systems, the interplay between the orbital filling and magnetism gives rise to a variety of magnetic phases. In iron superconductors, estimates for J_1 and J_2 have been restricted to a few ab-initio calculations for specific compounds [8, 9, 11–13]. The extraction of the exchange parameters from neutron experiments is still controversial [14–16]: An unexpected FM J_1 has been recently proposed to fit the spin-wave spectrum of iron chalcogenides [16].

In this letter we analyze the magnetic interactions of iron superconductors on the basis of a five orbital model [17] treated both within HF and Heisenberg approximations. We focus on the AF or FM character of the strong coupling exchange constants J_1 and J_2, on how they depend on the doping and on the Fe-As layer geometry, and check whether $(\pi, 0)$ is the actual ground state. We find that in undoped compounds J_1 and J_2 have a non-trivial dependence on the Fe-As-Fe angle and may become FM at large Hund's coupling J_H due to virtual transitions involving filled $3z^2 - r^2$ or $x^2 - y^2$ orbitals. FM tendencies are suppressed with hole-doping, but enhanced with electron-doping. The region of stability of the $(\pi, 0)$ state increases in HF with respect to the strong coupling predictions. An unusual orbital reorganization stabilizes (π, π) ordering in both HF and Heisenberg descriptions for a wide range of parameters. A DS state shows up at large U and J_H in the HF phase diagram. This DS state is charge modulated and unstable towards phase separation for $n = 6$ but it can be stabilized with electron doping.

The 5-orbital Hamiltonian includes intraorbital U and interorbital U', Hund's J_H and pair hopping J' terms.

$$\begin{aligned} H \; &= \sum_{i,j,\gamma,\beta,\sigma} t_{i,j}^{\gamma,\beta} c_{i,\gamma,\sigma}^{\dagger} c_{j,\beta,\sigma} + h.c. + U \sum_{j,\gamma} n_{j,\gamma,\uparrow} n_{j,\gamma,\downarrow} \\ &+ \; (U' - \frac{J_H}{2}) \sum_{j,\gamma>\beta,\sigma,\tilde{\sigma}} n_{j,\gamma,\sigma} n_{j,\beta,\tilde{\sigma}} - 2J_H \sum_{j,\gamma>\beta} \vec{S}_{j,\gamma} \vec{S}_{j,\beta} \\ &+ \; J' \sum_{j,\gamma\neq\beta} c_{j,\gamma,\uparrow}^{\dagger} c_{j,\gamma,\downarrow}^{\dagger} c_{j,\beta,\downarrow} c_{j,\beta,\uparrow} + \sum_{j,\gamma,\sigma} \epsilon_{\gamma} n_{j,\gamma,\sigma} \, . \end{aligned} \tag{1}$$

i, j label the Fe sites in the Fe unit cell, σ the spin and γ and β the five Fe d-orbitals yz, zx, xy, $3z^2 - r^2$ and $x^2 - y^2$, with x and y axis along the Fe-Fe bonds. The hopping amplitudes, restricted to first and second neighbors, depend on the angle α formed by the Fe-As bonds and the Fe-plane[17]. $\alpha = 35.3^o$, corresponding to the regular Fe-As tetrahedra, is assumed except when indicated. We use $U' = U - 2J_H$ [18], $J' = J_H$, and take [17] $\epsilon_{xy} = 0.02$, $\epsilon_{zx,yz} = 0$, $\epsilon_{3z^2-r^2} = -0.55$ and $\epsilon_{x^2-y^2} = -0.6$ for the crystal field. Energies are in units of $(pd\sigma)^2/|\epsilon_d - \epsilon_p| \sim 1$ eV, with $pd\sigma$ the σ overlap between the Fe-d and As-p orbitals and $|\epsilon_d - \epsilon_p|$ their energy difference[17]. For details on the mapping to a classical

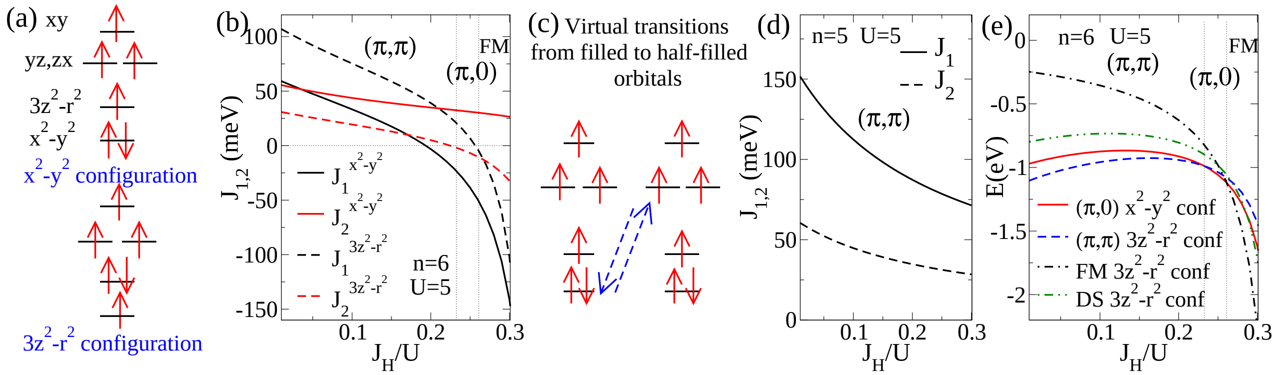

FIG. 1: (Color online) (a) Sketch of the two different orbital configurations ($\lambda = x^2 - y^2$ and $\lambda = 3z^2 - r^2$) of the $S = 2$ state for $n = 6$. (b) Exchange constants for $n = 6$, $U = 5$ eV, and $\alpha = 35.3^o$ as a function of Hund's coupling. (c) Illustration of the virtual transitions involving filled orbitals responsible for the FM exchanges for $n = 6$ at large J_H/U. (d) Exchange constants as a function of J_H/U for $n = 5$ and $U = 5$ eV assuming a $S = 5/2$ state. A (π,π) ground state is always favored. (e) Energies of the magnetic ground states as a function of J_H/U for the same parameters as in (b). The double stripe order, although never the ground state, is included for comparison. Vertical lines in (b) and (e) separate regions with different ground states $[(\pi,\pi), (\pi,0)$ and FM].

Heisenberg model and HF treatment see the supplementary information (SI) [19].

To second order in perturbation theory, starting from localized atomic states, the 5-orbital Hamiltonian is mapped onto a classical Heisenberg Hamiltonian:

$$E_0^{\{\lambda\}} + \frac{J_1^{\{\lambda\}}}{|S|^2} \sum_{\langle i,j \rangle} \vec{S}_i \vec{S}_j + \frac{J_2^{\{\lambda\}}}{|S|^2} \sum_{\langle\langle i,j \rangle\rangle} \vec{S}_i \vec{S}_j \qquad (2)$$

with $\vec{S}_i = \sum_\beta \vec{S}_{i,\beta}$ the atomic moment and $\langle i,j \rangle$ and $\langle\langle i,j \rangle\rangle$ restricted to first and second nearest neighbors respectively. We focus on the largest possible spin state, with each orbital being half-filled or filled. For $n = 6$, as in undoped compounds, this corresponds to $S = 2$. This large spin state dominates the $(\pi,0)$ mean field phase diagram at large U [20, 21]. Due to the small crystal field splitting, we consider two possible atomic configurations, labelled by $\{\lambda\}$, for the $S = 2$ state with filled $x^2 - y^2$ or $3z^2 - r^2$ orbitals, see Fig. 1 (a).

As expected, the exchange constants in both atomic configurations decrease monotonically with Hund's coupling, see Fig. 1(b). But the decrease is notably steep, mainly for J_1 and at large J_H/U, where a change in the slope happens and the exchange constants even become FM. This strong dependence at large J_H is due to virtual transitions from a filled orbital to a half-filled one on a neighbor atom, see Fig. 1(c) and SI [19]. These transitions are favored by the small crystal field splitting characteristic of iron pnictides. On the other hand, there are no filled orbitals at $n = 5$ in its highest spin state ($S = 5/2$), implying a weaker dependence on J_H/U of the exchange parameters, always AF, see Fig. 1(d). The opposite trend is found for $n = 7$, not shown, with two completely filled orbitals and enhanced FM behavior.

For $n = 5$, $J_2 < J_1/2$ and (π,π) ordering is found. For $n = 6$, in the $x^2 - y^2$ configuration, favored by the crystal field splitting, the $(\pi,0)$ state is lowest in energy, except at large J_H/U for which FM is expected. When comparing the energies between the ordered states in both orbital configurations in Fig. 1(e), the (π,π) order with filled $3z^2 - r^2$ becomes the ground state in a wide range of parameters. The selection of (π,π) in the $3z^2 - r^2$ configuration is in accordance with the exchange constants ratio $J_2^{3z^2-r^2} < J_1^{3z^2-r^2}/2$. Remarkably, the gain in magnetic energy, including E_0^λ, compensates for the cost in crystal field ($\epsilon_{3z^2-r^2} - \epsilon_{x^2-y^2} = 0.05$), see SI[19].

The appearance of (π,π) as the ground state is reproduced in the HF phase diagram in Fig. 2. As in the strong coupling picture, (π,π) in a $3z^2 - r^2$ configuration and $(\pi,0)$ in a $x^2 - y^2$ configuration dominate the phase diagram. In the $(\pi,0)$ state, $3z^2 - r^2$ is emptied while $x^2 - y^2$ gets filled as U increases [20]. In the (π,π) state, $3z^2 - r^2$ fills with increasing U while the other orbitals tend to half filling, see SI [19]. The transition between (π,π) and $(\pi,0)$ as J_H increases is accompanied by a charge transfer between $x^2 - y^2$ and $3z^2 - r^2$.

The $(\pi,0)$ state is more prominent in the HF phase diagram than in the Heisenberg description, specially close to the NM region. As previously found [20], two different $(\pi,0)$ states show up at the HF level. In the LM state, opposite orbital magnetizations within the same atom result in a low magnetic moment which violates Hund's rule. This state is stabilized thanks to the anisotropy of the orbital exchange constants [20] and has been proposed to explain the low magnetic moment found experimentally [20, 22, 23]. In the HM state, all the orbital magnetizations point in the same direction. The strong coupling predictions, dashed lines in Fig. 2, are valid for comparison with this HM state.

At large J_H the kinetic energy effects present at the HF level prevent the FM solution found in the strong coupling description to arise. Instead, a double stripe

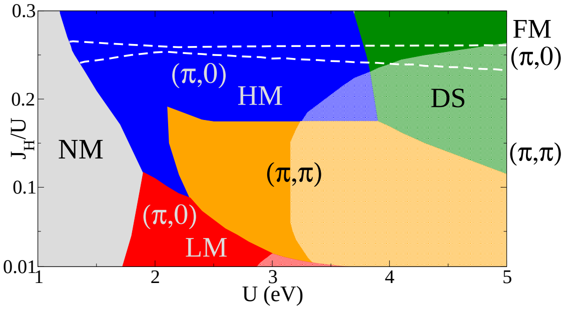

FIG. 2: (Color online) Hartree Fock magnetic phase diagram calculated at fixed density $n = 6$ as a function of U and J_H/U. Grey stands for non-magnetic (NM), blue for the AF $(\pi, 0)$ high moment (HM) state satisfying Hund's rule, red for a the AF $(\pi, 0)$ low moment (LM) state which violates Hund's rule, orange for AF (π, π) and green for the double stripe (DS) state with charge modulation (see text). Shaded areas mark insulating phases. Superposed dashed lines on the magnetic regions show the phase transition lines between the (π, π) and HM $(\pi, 0)$ states and between the HM $(\pi, 0)$ and the FM phase predicted by the $S = 2$ Heisenberg model.

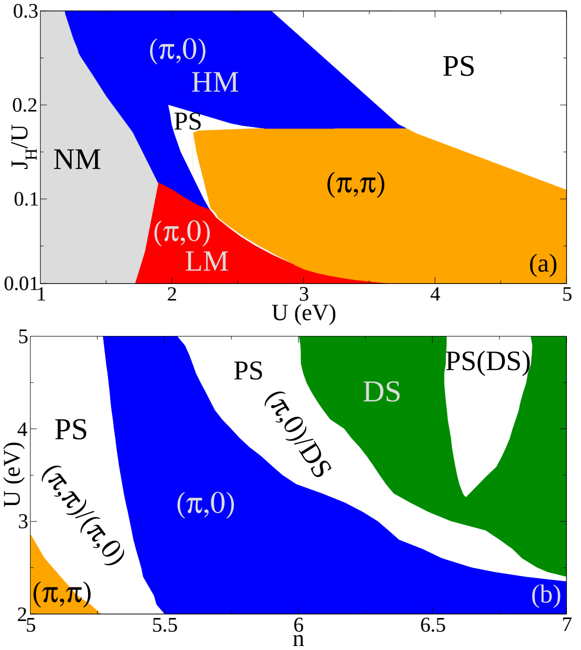

FIG. 3: (Color online) Mean field magnetic phase diagram in the grand canonical ensemble as a function of U and J_H/U and for $n = 6$ (a) and as a function of U and n for $J_H/U = 0.22$ (b). Same color code as in Fig. (2) applies. White regions are unstable towards phase separation.

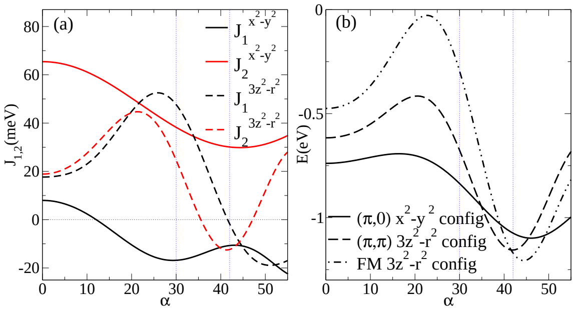

FIG. 4: (Color online) (a) First and second nearest neighbor exchange constants J_1^λ and J_2^λ as a function of α, the angle formed by the Fe-As bond and the Fe plane, for $n = 6$, $U = 5$ eV, and $J_H/U = 0.22$. (b) Energies of the most competitive magnetic orderings as a function of α for the parameters in (a). The sequence of magnetic orderings with increasing α is $(\pi, 0)$, (π, π), and FM. Vertical lines delimitate the experimentally relevant values of α.

solution is found at large U and J_H. This DS state is charge modulated (5 or 7 electrons for the $n = 6$ case) in a checkerboard fashion. Note that in the Heisenberg picture, a homogeneous DS state, though not the ground state, is lower in energy than both (π, π) and $(\pi, 0)$ at large J_H/U, see Fig. 1(e). The homogeneous DS state, with n electrons in each atom, is difficult to stabilize in the HF calculations, mainly at large J_H. When stabilized, it has larger energy than the charge modulated DS state. As shown in Fig. 3, the DS state is unstable towards phase separation at $n = 6$, see SI [19], but can be stabilized by electron doping. As expected for first order transitions, PS appears at the boundary between the different magnetic phases. The instability at $n \gtrsim 6.5$, which only involves the DS state, has a different origin: it is caused by a negative compressiblity related to the charge modulation.

Fig. 3(b) also evidences an electron-hole asymmetry around the undoped composition $n = 6$. In agreement with the strong coupling predictions, for $n = 5$ (π, π) correlations dominate, even at large J_H (calculations at $J_H/U = 0.28$ give similar results). When n increases, the $(\pi, 0)$ state becomes lower in energy, being the ground state in a wide region of parameters. For $n > 6$ and intermediate or large U the DS state is found. A larger tendency to DS solutions with increasing n is also expected in the Heisenberg description. Within HF, the electron-hole asymmetry close to $n = 6$ gets reduced as U decreases.

We finally analyze the effect of the Fe-As-Fe geometry on the magnetic interactions. A direct relation between the Fe-As-Fe angle and the critical superconducting temperature [2, 24, 25] as well as on the magnetic ordering [16] has been claimed. As illustrated in Fig. 4, the exchange constants vary non-monotonically with α due to the relative importance of the hopping (to both first and second neighbors) via the As [17]. The dependences of J_1 and J_2 on α are different for the $x^2 - y^2$ and $3z^2 - r^2$ configurations, with J_1/J_2 changing with α. For some values of α, J_1 ($J_1^{x^2-y^2}$ in special) and J_2 are FM. An alternance of magnetic states involving orbital reorganization, similar to the one discussed above, is found. For the value of J_H/U chosen, the transitions between these orders occur within the range of physical values of α, partly due to E_0^λ, see SI [19].

In summary, we have analyzed the magnetic interactions and ground state of a five orbital model for iron pnictides by means of a strong-coupling Heisenberg and a Hartree Fock approach. The tendency to $(\pi,0)$ ordering is enhanced in the mean field description, both in the large J_H region and in the small U region. The kinetic energy nesting properties of the Fermi surface may be important for the latter area, where HF is expected to give a better description and the resistivity shows anisotropic behavior consistent with experiment[21]. The value and sign of the exchange constants of the strong coupling model depend non-trivially on the Fe-As-Fe angle, the orbital filling, the number of electrons per Fe, and the Hund's coupling J_H. The small crystal field splitting characteristic of iron pnictides produces a strong decrease of the exchange constants with J_H and stabilizes an orbitally reorganized (π,π) state in a wide range of parameters, both for the weak and strong coupling descriptions. In the Heisenberg description, virtual transitions from filled to half-filled orbitals, of little importance in many materials because of large crystal field splittings, induce a strong tendency to FM at large J_H. FM is absent at the HF level, while a double stripe solution is found at large J_H/U. The system shows a strong tendency towards phase separation in the mean field approach, specially at large U and J_H/U, including a region with phase separation between $(\pi,0)$ and double stripe orderings. The double stripe state is charge modulated. Whether it is related to the state found in FeTe is at present not known.

Further conclusions can be obtained from this analysis. First, the exchange constants in the $(\pi,0)$ and (π,π) states may be different. Thus estimating these constants by comparing the energy of the different magnetic states with those predicted by a mapping to a Heisenberg model [8, 9, 12, 13] with the same J_1 and J_2 may lead to errors. Second, the orbital reorganization which accompanies the $(\pi,0)$-(π,π) transition implies an unexpected sensitivity of the ground state to the crystal field splitting $\epsilon_{3z^2-r^2}-\epsilon_{x^2-y^2}$. Most of the proposed tight binding models have very similar values for this splitting and similar physics is expected, although the quantitative details may depend on the parameters. Third, our results indicate that the filled orbitals are not inert for magnetism, so the use of 4-orbital models which neglect them to estimate the exchange parameters may be questionable [26].

Our results stress the relevance of Hund's coupling, also emphasized by other authors [11, 26–28]. At small values of J_H, Hund's rule may be violated resulting in a $(\pi,0)$ low magnetic moment state[20]. $(\pi,0)$ ordering is also favored at large J_H. A large J_H produces a strong decrease of the exchange constants, more important with electron doping, leading to small AF or even FM J_1 in the experimental range of parameters. These results could be relevant to understand the neutron scattering experiments.

We have benefited from conversations with F. Guinea, A. Chubukov and N. Perkins. We acknowledge funding from Ministerio de Ciencia e Innovación through Grants No. FIS 2008-00124, FIS 2009-08744 and Ramón y Cajal contract, and from CSIC through Grants No. PIE-200960I033 and PIE-200960I180.

---

[*] Electronic address: leni@icmm.csic.es

[1] C. de la Cruz, Q. Huang, J. Lynn, J. Li, W. Ratcliff, J. Zarestky, H. Mook, G. Chen, J. Luo, N. Wang, et al., Nature **453**, 899 (2008).

[2] J. Zhao, Q. Huang, C. de la Cruz, S. Li, J. Lynn, Y. Chen, M. Green, G. Chen, G. Li, Z. Li, et al., Nature Materials **7**, 953 (2008).

[3] I. Mazin, M. D. Johannes, L. Boeri, and K. Koepernik, Phys. Rev. B **78**, 085104 (2008).

[4] S. Raghu, X. Qi, C.-X. Liu, D. Scalapino, and S.-C. Zhang, Phys. Rev. B **77**, 220503 (2008).

[5] A. Chubukov, D. Efremov, and I. Eremin, Phys. Rev. B **78**, 134512 (2008).

[6] Q. Si and E. Abrahams, Phys. Rev. Lett. **101**, 076401 (2008).

[7] T. Yildirim, Physical Review Letters **101**, 057010 (2008).

[8] F. Ma, W. Ji, J. Hu, Z.-Y. Lu, and T. Xiang, Phys. Rev. Lett. **102**, 177003 (2009).

[9] C.-Y. Moon and H. J. Choi, Phys. Rev. Lett. **104**, 057003 (2010).

[10] Y. Xia, D. Qian, L. Wray, D. Hsieh, G. F. Chen, J. L. Luo, N. L. Wang, and M. Z. Hasan, Phys. Rev. Lett. **103**, 037002 (2009).

[11] K. Haule and G. Kotliar, New Journal of Physics **11**, 025021 (2009).

[12] C.-Y. Moon, S. Y. Park, and H. J. Choi, Phys. Rev. B **80**, 054522 (2009).

[13] X.-W. Yan, M. Gao, Z.-Y. Lu, and T. Xiang, arXiv:1012.5536.

[14] J. Zhao, D. T. Adroja, D.-X. Yao, R. Bewley, S. Li, X. F. Wang, G. Wu, X. H. Chen, J. Hu, and P. Dai, Nature Physics **5**, 555 (2009).

[15] A. Wysocki, K. Belashchenko, and V. P. Antropov, Nature Physics **7**, 485 (2011).

[16] J. Hu, B. Xu, W. Liu, N.-N. Hao, and Y. Wang, arXiv:1106.5169.

[17] M. J. Calderón, B. Valenzuela, and E. Bascones, Phys. Rev. B **80**, 094531 (2009).

[18] C. Castellani, C. R. Natoli, and J. Ranninger, Phys. Rev. B **18**, 4945 (1978).

[19] See supplementary information.

[20] E. Bascones, M. J. Calderón, and B. Valenzuela, Phys. Rev. Lett. **104**, 227201 (2010).

[21] B. Valenzuela, E. Bascones, and M. J. Calderón, Phys. Rev. Lett. **105**, 207202 (2010).

[22] F. Cricchio, O. Granas, and L. Nordstrom, Phys. Rev. B **81**, 140403 (2009).

[23] G.-Q. Liu, arXiv:1105.5412v1 (2011).

[24] C. H. Lee, A. Iyo, H. Eisaki, H. Kito, M. T. Fernandez-Diaz, T. Ito, K. Kihou, H. Matsuhata, M. Braden, and K. Yamada, J. Phys. Soc. Jpn. **77**, 083704 (2008).

[25] K. Kuroki, H. Usui, S. Onari, R. Arita, and H. Aoki, Phys. Rev. B **79**, 224511 (2009).

[26] P. Hansmann, R. Arita, A. Toschi, S. Sakai, G. Sangio-

vanni, and K. Held, Phys. Rev. Lett. **104**, 197002 (2010).
[27] Z. P. Yin, K. Haule, and G. Kotliar, Nature Physics **7**, 294 (2010).
[28] M. Johannes and I. Mazin, Phys. Rev. B **79**, 220510R (2009).

Supplementary Information

Here we provide the details of the calculations we refer to in the text. Starting from localized atomic states we map the 5-orbital interacting Hamiltonian of Eq.(1) in a classical Heisenberg Hamiltonian with exchange interactions to first and second nearest neighbors

$$E_0^{\{\lambda\}} + \frac{J_1^{\{\lambda\}}}{|S|^2} \sum_{\langle i,j \rangle} \vec{S}_i \vec{S}_j + \frac{J_2^{\{\lambda\}}}{|S|^2} \sum_{\langle\langle i,j \rangle\rangle} \vec{S}_i \vec{S}_j \ . \tag{S1}$$

Here λ labels the considered orbital configuration (as defined in Fig. 1 (a)), $\vec{S}_i = \sum_\beta \vec{S}_{i,\beta}$ the atomic moment and $\langle i,j \rangle$ and $\langle\langle i,j \rangle\rangle$ are restricted to first and second nearest neighbors respectively. We restrict to atomic states with maximum total spin S ($S=2$ for $n=6$ and $S=5/2$ for $n=5$) and maximum $|S_z|$ ($S_Z=\pm 2$ and $S_z=\pm 5/2$ for $n=6$ and $n=5$ respectively). With this, $E_0^{\{\lambda\}}$ and $J_{1,2}^{\{\lambda\}}$ are

$$E_0^\lambda = \sum_{\langle i,j \rangle, \langle\langle i,j \rangle\rangle} \frac{E^{\{\lambda\}}_{FM;i,j} + E^{\{\lambda\}}_{AF;i,j}}{4} \tag{S2}$$

$$J_{1,2}^\lambda = \frac{E^{\{\lambda\}}_{FM;i,j} - E^{\{\lambda\}}_{AF;i,j}}{4} \tag{S3}$$

with i,j two first (second) nearest neighbors for J_1 (J_2). $E^{\{\lambda\}}_{FM;i,j}$ and $E^{\{\lambda\}}_{AF;i,j}$ are the energies corresponding to two parallel or antiparallel spins at i and j. The factor of 4 (instead of 2) corrects the bond double-counting in Eq.(S1). When using Eqs. (S2) and (S3) we are neglecting quantum fluctuations. In this sense we are treating the spin classically. As discussed in the text and below, the classical approximation provides good understanding on the magnetic interactions dominant in iron pnictides. Quantum fluctuations are expected to be of little importante for large spins. Spin states $S=2$ and $S=5/2$ discussed in the text are large enough to justify the classical treatment of spins.

FM and AF energies can be written in terms of atomic and magnetic energies

$$E^{\{\lambda\}}_{FM,AF;i,j} = E^{\{\lambda\}}_{at} + E^{\{\lambda\},mag}_{FM,AF;i,j} \tag{S4}$$

where $E^{\{\lambda\}}_{at}$ accounts for the interaction and crystal field energy to charge the atoms to the $n=6$ or $n=5$ state selected, while $E^{\{\lambda\},mag}_{FM,AF;i,j}$ is the magnetic contribution. $E^{\{\lambda\}}_{at}$ enters in the value of the constant $E_0^{\{\lambda\}}$ but cancels out in the expression of the exchange constants $J_{1,2}^{\{\lambda\}}$. We simplify $E^{\{\lambda\}}_{at}$ to $E^{x^2-y^2}_{at}=0$ and $E^{3z^2-r^2}_{at} = \epsilon_{3z^2-r^2} - \epsilon_{x^2-y^2}$ per atom, as the other terms drop out from the calculation. For $n=6$

$$E^{\{\lambda\},mag}_{AF;i,j} = -\sum_{\eta,\nu} \frac{2(t^{\nu,\eta}_{i,j})^2}{J'^2+\Delta E_-^2} \left(\frac{\Delta E_-^2}{U+3J_H+\epsilon_\eta-\epsilon_\nu+\Delta E_+} + \frac{J'^2}{U+3J_H+\epsilon_\eta-\epsilon_\nu+\Delta E_-} \right) - \sum_\nu 2(t^{\lambda,\nu}_{i,j})^2 \left(\frac{1/5}{U-3J_H+\epsilon_\eta-\epsilon_\lambda} + \frac{4/5}{U+2J_H+\epsilon_\eta-\epsilon_\lambda} \right) \tag{S5}$$

Here η and ν label half-filled orbitals and λ refers to the filled one; $t^{\beta\gamma}_{i,j,}$ are the hopping amplitudes between orbitals β and γ in atoms i and j respectively[17]. $\Delta E_\pm = \epsilon_\nu - \epsilon_\lambda \pm \left((\epsilon_\lambda-\epsilon_\nu)^2 + J'^2\right)^{1/2}$. The first term in Eq. (S5) includes virtual transition from half-filled orbitals in one atom to half-filled orbitals in a neighbour atom and takes into account that the intermediate state is not an eigenstate of the pair hopping operator. The second term is associated with virtual transitions of an electron from the filled orbital to a half-filled orbital in the other atom. Only the electron whose spin is opposite to the magnetic moment of the neighbor atom can hop. The state left behind is not an eigenstate of the Hund's term.

When the magnetic moments of the two atoms are parallel the only transitions allowed involve the filled orbital. The contribution of these transitions is

$$E^{\{\lambda\},mag}_{FM;i,j} = -\sum_\nu \frac{2(t^{\lambda,\nu}_{i,j})^2}{U-3J_H+\epsilon_\lambda-\epsilon_\nu} \tag{S6}$$

For $n=5$ and $S=5/2$ $E^{S=5/2,mag}_{FM;i,j}=0$ and

$$E^{S=5/2,mag}_{AF;i,j} = -\sum_{\nu\eta} \frac{2(t^{\eta,\nu}_{i,j})^2}{U+4J_H+\epsilon_\eta-\epsilon_\nu} \tag{S7}$$

In this latter case, the exchange constants are clearly AF. Whether a (π,π) or $(\pi,0)$ state is favoured depends on the relative values of J_1 and J_2. As shown in Fig. 1, (π,π) ordering is always preferred.

The $n=6$ case is more interesting. For $J_H=0$ the contribution of the transitions which depart from filled orbitals is the same with FM or AF ordering. Consequently they do not affect the magnetic ordering, and the exchange constants, driven by the transitions from half-filled orbitals are AF. With increasing J_H their contribution is larger in the FM case. At a given J_H these transitions favor FM ordering. For small J_H the transitions from half-filled orbitals still dominate, but at large J_H J_1^λ and J_2^λ become ferromagnetic. Due to different

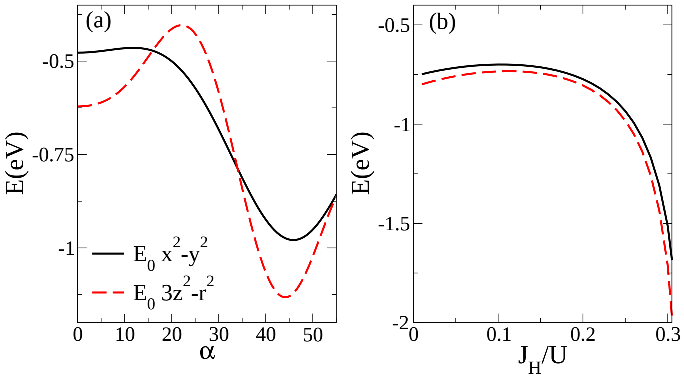

FIG. S1: (Color online) Dependence of $E_0^{x^2-y^2}$ and $E_0^{3z^2-r^2}$ for $n = 6$ and $U = 5$ eV as a function of the Fe-As-Fe angle α for $J_H/U = 0.22$ (a) and Hund's coupling for $\alpha = 35.3^o$(b).

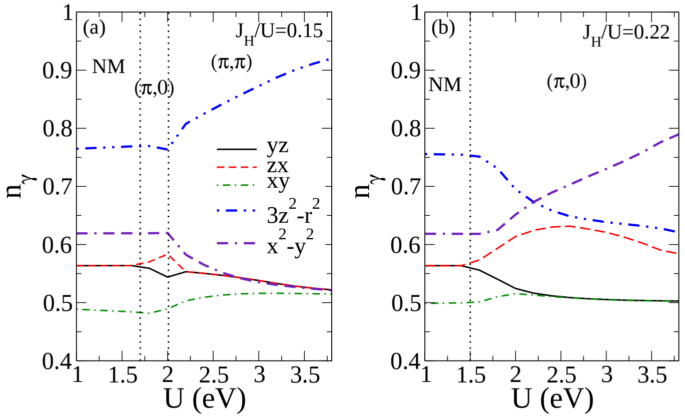

FIG. S2: (Color online) (a) and (b) Dependence of the orbital filling as a function of the intraorbital interaction for $J_H/U = 0.15$ and $J_H/U = 0.22$ respectively. Vertical lines separate regions with different ground states.

$t_{i,j}^{\gamma\beta}$ in each of these terms the value of J_H at which this happens is different for each exchange constant.

Another interesting aspect regards $E_0^{\{\lambda\}}$. The contribution of $E_{FM,AF;i,j}^{\{\lambda\},mag}$ to $E_0^{\{\lambda\}}$ can be seen as the energy gain associated to creating magnetic moments, even if on average they do not order. When mapping to Heisenberg models it is usual to disregard E_0 because if a single atomic state is selected its value does not affect the differences in energy between magnetic states. However, for $n = 6$, the small crystal field splitting between $x^2 - y^2$ and $3z^2 - r^2$ requires the inclusion of two different atomic states. Due to different hopping amplitudes involving these orbitals, $E_0^{x^2-y^2} \neq E_0^{3z^2-r^2}$ is found. This can be observed in Fig. S1 as a function of the Fe-As-Fe and Hund's coupling. Consequently $E_0^{\{\lambda\}}$ helps select the atomic state $\{\lambda\}$, with the a priori unexpected result that the atomic state in which $3z^2 - r^2$ is filled is preferred in a wide range of parameters. Note that the formation of magnetic moments is favoured in the experimentally relevant range of Fe-As-Fe angle and at large Hund's coupling. The large values of $E_0^{\{\lambda\}}$ also explain the large values of the total energy, despite the relatively small values of the exchange constants.

We have compared these predictions with a self-consistent mean-field Hartree Fock calculation which includes non-magnetic (NM), FM, and AF states with $Q = (\pi, 0)$, $Q = (\pi, \pi)$, and DS ordering. In the DS calculation the system is divided into two interpenetrating lattices coupled via first nearest neighbor hopping terms. The axis and orbital basis is rotated and a $(\pi, 0)$ state along the Fe-diagonals is assumed. In the mean-field calculation only spin and orbital-diagonal average terms are kept:

$$\begin{aligned} n_\gamma &= \sum_{k,\sigma} \langle c^\dagger_{k,\gamma,\sigma} c_{k,\gamma,\sigma} \rangle \qquad \text{(S8)} \\ m_\gamma &= \sum_{k} \left[\langle c^\dagger_{k+\mathbf{Q},\gamma,\uparrow} c_{k,\gamma,\uparrow} \rangle - \langle c^\dagger_{k+\mathbf{Q},\gamma,\downarrow} c_{k,\gamma,\downarrow} \rangle \right] . \end{aligned}$$

We have checked that this approximation does not have any influence on the mean field results. Terms disregarded are of order $\sim 10^{-4}$. Several initial configurations for n_γ and m_γ are probed for each ordered state. A self-consistent solution is considered to be ordered (insulating) when the magnetic moment m (gap) is larger than 0.001. Fig. 2 shows the phase diagram corresponding to $n = 6$ calculated at fixed density. The mean field ground state evolves from a non-magnetic solution with zero magnetic moment and orbital fillings close to the non-interacting ones at small U to $(\pi, 0)$ and (π, π) states with $m = 4\mu_B$, with μ_B a Bohr magneton, as in an atomic $S = 2$ state at large U. As seen in Fig. S2 every orbital except $x^2 - y^2$ tends to half filling at large U, $x^2 - y^2$ becoming completely filled, in the $(\pi, 0)$ state. This orbital filling is expected on the basis of the crystal field splitting. On the other hand, in the (π, π) state, it is the $3z^2 - r^2$ orbital the one which fills completely while $x^2 - y^2$ tends to half-filling. This orbital filling competes with the crystal field, in agreement with the strong coupling predictions, see main text.

The phase diagram in Fig. 2 has been obtained comparing the energies of the mean-field solutions at fixed density. Different phases have a different energy E versus density n relation. Jumps of the chemical potential μ appear at first-order boundaries between ordered phases. In such situations phase separation is expected. In a range of densities the system decreases its energy by allowing relative fractions of the two neighboring magnetic phases. $n = 6$ may belong to this range of densities for values of the interactions close to phase boundaries. To determine the region of phase space unstable towards phase separation in Fig. 3 we work in the grand-canonical ensemble (fixed chemical potential) and compare $E - \mu n$ for the different states. The chemical potential can be calculated as $\partial E/\partial n$ or by looking at the energy of the last state occupied in metallic systems, both methods giving the same value. μ jumps discontinuously when crossing a gap. According to Maxwell's construction phase boundaries between two phases 1 and 2 are given by $E_1 - \mu n_1 = E_2 - \mu n_2$. Neither phase 1 nor phase 2 are stable in the range $n_1 < n < n_2$. A phase separated mixture of both phases arises.

Phase separation for a given phase will also appear with negative compressibility , i.e. μ decreases with increasing n. This is observed in the DS state in several ranges of n, including $n = 6$ and $n \leq 6.5$. In this case phase separation happens between states with the same magnetic ordering but different density. Densities n_1 and n_2 are determined as above. Note, that while at $n = 6$ DS is intrinsically unstable towards phase separation, at this density phase separation between DS and $(\pi, 0)$ is favored.